PHYSICAL REVIEW B VOLUME 41, NUMBER 5 15 FEBRUARY 1990-I

Auger and electron-energy-loss spectroscopy study of interface formation in the Ti-Si system

X. Wallart, J. P. Nys, H. S. Zeng, G. Dalmai, I. Lefebvre, and M. Lannoo
Laboratoire d'Etude des Surfaces et Interfaces, U.R.A. D0253,
Institut Supérieur d'Electronique du Nord, 41 boulevard Vauban, 59046 Lille CEDEX, France
(Received 3 August 1989)

We present a detailed study of interface formation in the titanium-silicon (Ti-Si) system under different temperature conditions. We make use of electronic-structure calculations in order to interpret the silicon Si $L_{2,3}VV$ Auger line shape and the electron-energy-loss spectra. These techniques, together with low-energy electron diffraction and electron-microscopy observations and film-resistance data, allow us to discuss accurately the interface reactivity of the Ti-Si system with respect to temperature.

I. INTRODUCTION

The titanium-silicon and titanium silicide-silicon interfaces have attracted considerable interest in recent years due to the suitability of the disilicide $TiSi_2$ for microelectronics applications. $TiSi_2$ has the lowest resistivity among the refractory-metal silicides and so it is a promising material for interconnections and contacts. In the past, most studies have focused on the formation of thick (>1000 Å) $TiSi_2$ films.[1,2] However, due to the strong reactivity of titanium with impurities such as oxygen or carbon, results are sometimes contradictory and an overall agreement between them is difficult to find. Moreover, there are less studies concerned with thin films and interface formation so that the different interfaces formed in the system still remain incompletely characterized. Finally, in thin-film studies, disagreement can be noted between results derived from Auger-electron spectroscopy (AES) (Refs. 3 and 4) and those derived using other techniques.[5,6] In this work, we show that a careful quantitative and line-shape analysis of Auger spectra combined with theoretical calculations and other surface sensitive techniques can improve this situation and lead to a better understanding of the interfaces under study.

In a general way and in spite of Lander's suggestion[7] that core-valence-valence Auger spectra can reflect the self-folding of the valence density of electronic states (DOS), line-shape analysis of Auger transitions involving valence electrons is rarely performed. However, this is not the case for the silicon Si $L_{2,3}VV$ which has been extensively studied in the past in the case of clean Si(111) and Si(100) surfaces.[8–11] From this work, it is clear that hole-hole interactions in the final state of the Si $L_{2,3}VV$ transition are weak relative to the bandwidth[11] and so one can expect that interpretations of the Auger line shape in terms of noninteracting DOS to be adequate.[12] The second important conclusion arising from previous work is that the Auger matrix element varies strongly across the valence band[10] in such a way that interpretation of experimental spectra implies a predominant contribution of p-p processes (two p-like holes in the final state) over s-p and s-s processes[9,11] and leads to the use of s and p partial densities of states in order to interpret Si $L_{2,3}VV$ Auger spectra. An explanation of this matrix element variation has been given by Jennison[13] based on "atomic" and "bonding" charge concepts.

Concerning metal-silicon and silicide-silicon interfaces, the Si $L_{2,3}VV$ Auger line has been used in a number of systems: Pd-Si,[14,15] Ni-Si,[16] V-Si,[17] Cu-Si,[18] Au-Si,[19] Ca-Si.[20,21] In these cases, the experimental Auger spectra have rarely been properly treated in order to recover the basic Auger line and so the interpretation in terms of the DOS of the different silicides has been performed in a more or less qualitative way. Nevertheless, all these studies have shown the validity and the usefulness of the Si $L_{2,3}VV$ line-shape analysis to get reliable information on the local chemical environment at the interface. However, concerning the silicon line shape, there is little information available in the literature related to the Ti-Si system.

In this study, we investigate interface formation in the Ti-Si system under three different temperature conditions: (1) deposition of titanium on crystalline silicon at room temperature, (2) annealing of 70-Å-thick titanium films in the range 200–700 °C, and (3) deposition of titanium on heated crystalline silicon substrates. In each case, we discuss the silicon Si $L_{2,3}VV$ Auger line shape (ALS) obtained after a proper treatment of the experimental spectra in correlation with theoretical line shapes built with the theoretical DOS calculated for various compounds. These DOS are also used in order to interpret electron-energy-loss spectra (ELS). The overall agreement we obtain completed with microscopy and electron diffraction observations allows us to get a clear insight in the interface formation.

In the following, we first present the experimental procedure and results. We then give a detailed description of the method involved in the calculation of the various DOS before making use of them in the discussion and interpretation of our results.

 ©1990 The American Physical Society

II. EXPERIMENTAL

In this study, we have worked under ultrahigh vacuum with a base pressure around 2×10^{-10} Torr. Clean silicon substrates have been obtained by a chemical treatment according to the Shiraki method,[22] followed by a Joule annealing at 850–900 °C in ultrahigh vacuum. Titanium has been deposited by sublimation from a directly Joule heated filament onto clean Si(100) or Si(111) substrates.

AES and ELS spectra have been recorded with a hemispherical analyzer. For Auger spectra we worked in the direct mode, whereas for ELS spectra we used the second derivative mode as usual for this spectroscopy. The overall experimental resolution in these conditions is about 0.6 eV.

The experimental Si $L_{2,3}VV$ Auger line shapes have been corrected for secondary background using the empirical formula of Sickafus[23] with classical least-squares fitting procedure. Energy-loss processes have been taken into account by deconvolution of the Auger spectra with an energy-loss function recorded in the same conditions and at the Auger energy using the Van Cittert iterative method.[24,25] The line shapes obtained after this treatment should then essentially reflect the Auger emission process and allow a better comparison with theoretical calculations.

Finally, quantitative Auger analysis has been performed using the peak-to-background ratios in the direct mode.[26] For the calculation of Auger intensities related to some particular growth mode or compound, we have estimated the attenuation lengths with the empirical formula of Seah and Dench,[27] which gives essentially the same values as that of Powell.[28] The appropriate corrections for density changes from a material to an other have been performed as discussed elsewhere.[29]

III. RESULTS

A. Interface formation at room temperature

During titanium deposition at 25 °C, we note a strong change of the Si $L_{2,3}VV$ ALS (Fig. 1) consisting essentially of the appearance of a shoulder and then a peak at $\simeq 6$ eV from the main peak. This is not consistent with the growth of a pure titanium film which could not induce such a strong extra feature. In Fig. 2, we show the evolution of the experimental Ti LMM and Si LVV Auger intensities with increasing titanium coverage together with the calculated intensities for a layer-by-layer two-dimensional (2D) and a three-dimensional (3D) (according to a Poisson distribution) growth of pure titanium. From the comparison between the experimental and calculated intensities, it is clear that the growth of pure titanium cannot explain the experimentally observed intensities. Finally, Fig. 3 emphasizes the changes in the ELS spectra with Ti deposition. These spectra have been recorded with a primary energy of 200 eV for which the electron attenuation length is small (between 5 and 10 Å) and allows us to be very sensitive to modifications in the surface layer. The spectrum for pure silicon is similar to those reported before[30] with two surface transitions at 8 (S_2) and 15 eV (S_3), two bulk transitions at 3.5 (E_1) and 5 eV (E_2), and the volume and surface plasmons around 17 and 11 eV, respectively. The pure titanium spectrum obtained after deposition of 85×10^{15} atoms/cm^2 ($\simeq 150$ Å with 1 Å$\simeq 0.56\times10^{15}$ atoms/cm^2 for Ti) is characterized by two transitions at 5 and 8.5 eV, a surface plasmon energy around 12 eV, and a volume plasmon energy near 18 eV in good agreement with previous work.[31] During Ti deposition, the main changes are related to the shift of the volume and surface plasmons towards 18.5–19 eV and 12.5–13 eV, respectively, up to a deposited amount of 5×10^{15} atoms/cm^2 and then a shift backwards to the values of pure titanium. On all spectra, we always note transitions near 3.5 and 5 eV. Concerning the 8- and 15-eV transitions, they first disappear for low coverage ($<0.51\times10^{15}$ atoms/cm^2) and then a feature reappears near 7.5 eV and finally shifts to 8.5 eV in pure titanium. Table I displays the calculated values of the plasmon energies for different compounds in the Ti-Si system within the free-electron-gas approximation.[32] According to this and taking in account the uncertainties introduced by the

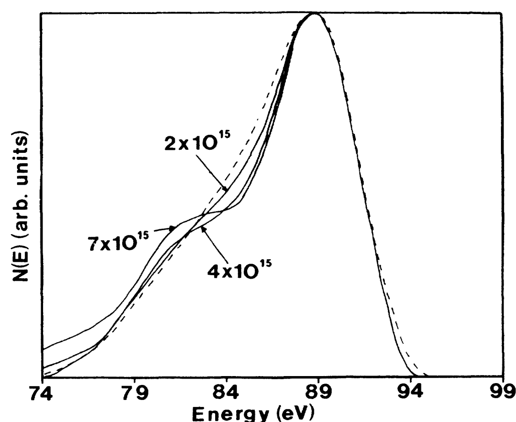

FIG. 1. Si $L_{2,3}VV$ Auger line shapes after deposition of 2×10^{15}, 4×10^{15}, and 7×10^{15} Ti atoms/cm^2 at room temperature on Si(111). Dashed lines, the line shape in pure silicon.

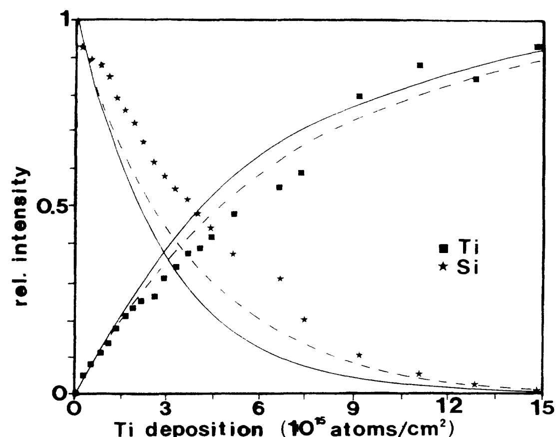

FIG. 2. Evolution of the Si LVV and Ti LMM Auger intensities during room-temperature deposition of titanium. Solid line, simulation of a layer by layer growth of pure titanium; dashed line, simulation of a 3D growth of pure titanium.

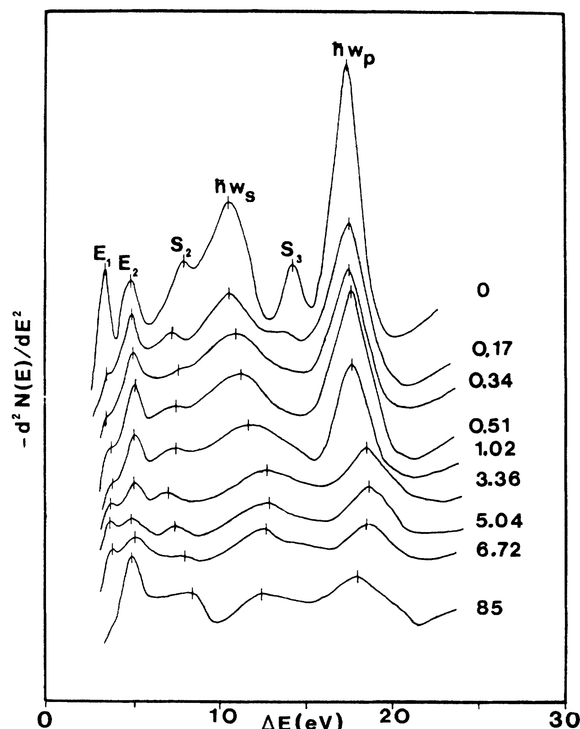

FIG. 3. Evolution of the ELS spectra during room-temperature deposition of titanium ($E_p = 200$ eV) with respect to the deposited amount of titanium (in 10^{15} atoms/cm^2).

approximation used and experimental resolution, the values we measure at low coverages ($<5\times10^{15}$ atoms/cm^2) seem to be related to the formation of TiSi and/or Ti_5Si_3.

From all these results—Si $L_{2,3}VV$ line-shape changes, Ti and Si Auger intensities, ELS spectra—it is clear that there is an interfacial reaction and formation of interfacial compounds. From ELS spectra, it can be deduced that this reaction extends to a Ti-deposited amount around 5×10^{15} atoms/cm^2 and probably leads to the formation of TiSi and/or Ti_5Si_3.

B. Annealing of 70-Å-thick Ti films

Figure 4 describes the evolution of Ti *LMM* and Si *LVV* Auger intensities during isochronal annealing of a 70-Å-thick Ti film in the temperature range 200–700 °C. We choose a 50 °C temperature step and an annealing

TABLE I. Calculated values of plasmons energies in the free-electron-gas approximation for various compounds in the Ti-Si system.

Compound	$\hbar\omega_p$ (eV)	$\hbar\omega_s$ (eV)
Si	16.6	11.7
$TiSi_2$	19.7	13.9
TiSi	19.4	13.7
Ti_5Si_3	18.8	13.3
Ti	17.7	12.5

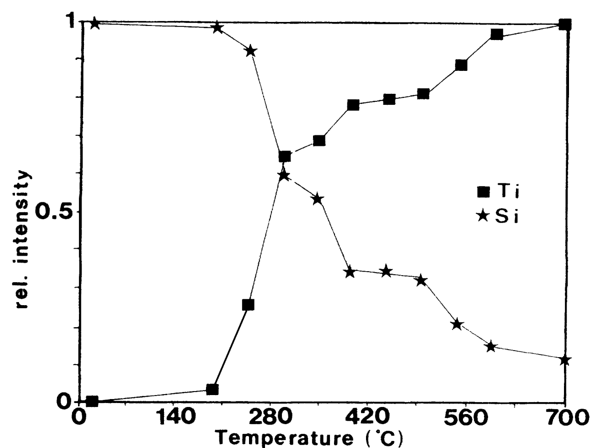

FIG. 4. Evolution of the Si *LVV* and Ti *LMM* Auger intensities during the annealing of a 70-Å-thick Ti film deposited at 25 °C.

time of 10 min at each step. On these curves, one can distinguish three different regions. For temperatures between 200 and 300 °C, the Auger intensities vary rapidly and this can be related to interdiffusion phenomena. When the temperature lies between 400 and 500 °C, the intensities remain unchanged, which indicates that the film has been converted into a stable compound. Then when $T > 500$ °C, one can note again an increase (decrease) of the silicon (titanium) Auger intensity. We have also measured *in situ* the variation of the film resistance during the annealing (Fig. 5). A similar distinction between three temperature ranges can be done on this curve mainly characterized by a strong minimum around 400–500 °C. We are now going to present detailed results on these three regions.

1. Annealing for $T \simeq 300$ °C

For this temperature, the Ti *LMM* and Si *LVV* Auger intensities are near those expected for TiSi (Fig. 4).[29] The final Si $L_{2,3}VV$ ALS (Fig. 6) presents only a weak shoul-

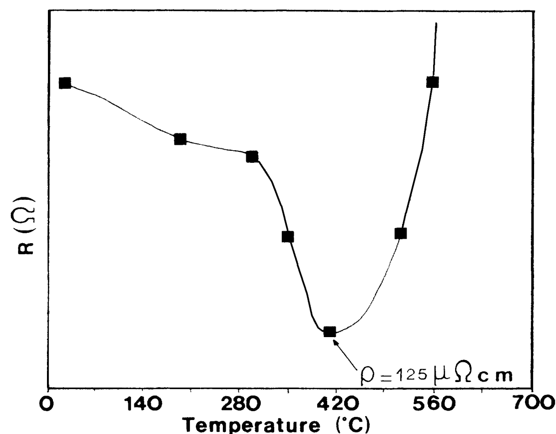

FIG. 5. Variations of the film resistance during the annealing of a 70-Å-thick Ti film deposited at 25 °C.

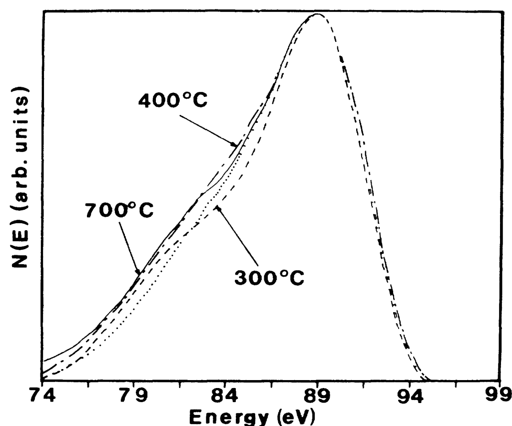

FIG. 6. Si $L_{2,3}VV$ Auger line shape after annealing of a 70-Å-thick Ti film at different temperatures. Dotted line, Si $L_{2,3}VV$ line shape in pure silicon.

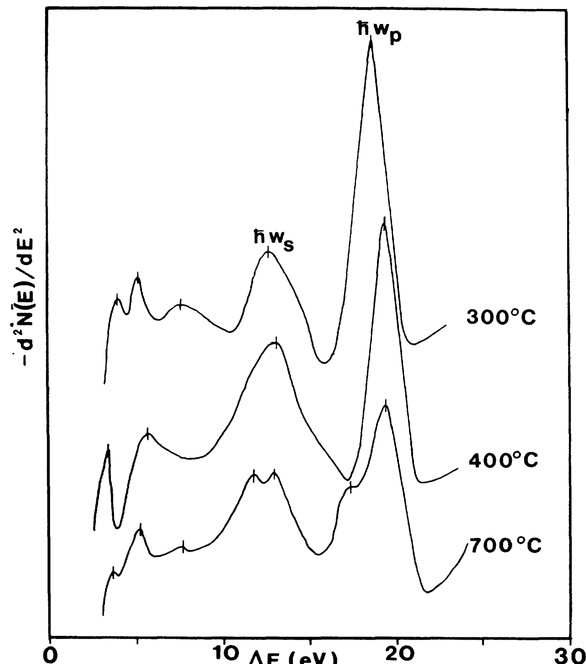

FIG. 7. ELS spectra after annealing of a 70-Å-thick Ti film at different temperatures ($E_p = 400$ eV).

der at $\simeq 6$ eV from the main peak. ELS spectra at different primary energies exhibit three electronic transitions around 3.5, 5, and 7.5 eV. The plasmon energy values are 19 and 13 eV for bulk and surface plasmons, respectively (Fig. 7). At last, the silicon Si *KLL* Auger line presents a clearly visible shift of 1–1.5 eV. This Auger line involves only core levels and so an energy shift of this transition is associated with changes in the atom electronic configuration indicative of the formation of compounds. All these results suggest that in this temperature range the whole film has reacted with the mean composition of the resulting compound being near that of TiSi.

2. *Annealing for 400 < T < 500 °C*

The film composition deduced from the Auger intensities (Fig. 4) is near that of $TiSi_2$. The Si $L_{2,3}VV$ ALS obtained in this case (Fig. 6) does not exhibit any particular structure but is broader than that in pure silicon. ELS spectra at different primary energies (Fig. 7) show two transitions at 3.5 and 5 eV but no more transition at 7.5 eV, in opposition with the previous case. Plasmon energies are now 19.5 and 13.5 eV, i.e., a bit higher than in the 300 °C case and in good agreement with the calculated values for $TiSi_2$ (Table I). The silicon Si *KLL* Auger line exhibits again a shift of 1–1.5 eV. Concerning resistance measurements, this temperature range is characterized by a strong minimum.

3. *Annealing for T > 500 °C*

In this last case, the Auger intensities are between those expected for $TiSi_2$ and those in pure silicon. The Si $L_{2,3}VV$ ALS is intermediate between that in pure silicon and that reported in the 400–500 °C annealing case (Fig. 6). On the ELS spectra (Fig. 7), we can observe double plasmon losses at 19.5 and 17 eV and 13.5 and 11 eV for bulk and surface plasmons, respectively. Moreover, apart from the 3.5- and 5-eV transitions, we note the appearance of a transition around 8 eV. Finally, low-energy electron diffraction (LEED) observations show the characteristic diagrams of the substrates, Si(111) or Si(100), with the corresponding reconstruction, (7×7) or (2×1), respectively.

C. Deposition of Ti on heated Si substrates

Another way of obtaining silicide formation is the deposition of Ti on a directly heated Si substrate[33] in such a way as to promote silicide formation during Ti deposition without any further annealing. We present here results relative to a substrate temperature of 400 °C.

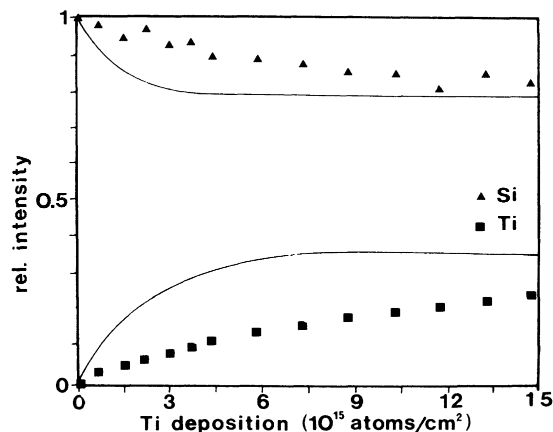

FIG. 8. Evolution of the Si *LVV* and Ti *LMM* Auger intensities during deposition of Ti on a 400 °C heated silicon substrate. Solid line, simulation of a layer by layer growth of $TiSi_2$.

TABLE II. Atomic energies from Ref. 35.

in eV	E_s	E_p	E_d
Si	−14.24	−7.03	
Ti			−4.86

The Ti *LMM* and Si *LVV* Auger intensities evolution during Ti deposition cannot be explained by a 2D growth of $TiSi_2$, as illustrated in Fig. 8, but rather suggests a 3D growth of $TiSi_2$. The Si $L_{2,3}VV$ ALS is similar to that of the annealing case for $T>500\,^{\circ}\mathrm{C}$ (Fig. 6), intermediate between that in pure silicon and that in the 400–500 °C annealing case. ELS spectra are essentially similar to those obtained for an annealing above 500 °C (Fig. 7) with double plasmon losses at 17 and 19.5 eV and 11 and 13.5 eV for volume and surface plasmons, respectively. Finally, a dark field transmission microscopy observation using the Moiré technique[34] has been performed after deposition of 23×10^{15} atoms/cm^2 ($\simeq 40$ Å). Analysis of these Moiré patterns reveals the growth of so-called $C49$ $TiSi_2$ grains in local epitaxy on the substrate.[34]

IV. THEORETICAL CONSIDERATIONS

In order to get insight in the local chemical environment, we have calculated the densities of electronic states in the valence band (DOS) for the three well-known silicides: Ti_5Si_3, TiSi, and $TiSi_2$ in its $C54$ and $C49$ structure. Because of the complex atomic structure of $TiSi_2$ and Ti_5Si_3 (Ref. 35) and the large number of atoms per unit cell (24 for $TiSi_2$ in its $C54$ structure), we have chosen the empirical tight-binding theory. In this method, the wave function is expressed as a linear combination of atomic orbitals (LCAO theory). We make use of a "minimal basis set" including only external valence states of the corresponding atoms, i.e., *s* and *p* for Si and *d* states for Ti. In the tight-binding approximation, the atomic states are considered to be orthogonal and, in its empirical version, the elements of the Hamiltonian matrix are parameters transferred from well-known cases.

These parameters are atomic energies for the diagonal elements of the Hamiltonian and hopping integrals for the others. We assume that atomic energies are those of the free atoms in the configuration s^2p^2 for Si and d^3s^1 for Ti whose values are calculated with the Herman and Skillman method[36] (Table II). The hopping integrals are taken to obey a two-center approximation.[37] In this type of calculation, interactions are usually limited to first-nearest neighbors, but in these compounds, it is necessary to take the following points into account.

(i) There is a distribution of close-neighbors distances for $TiSi_2$ in its $C54$ phase (2.54–2.75 Å) and for Ti_5Si_3 (2.63–3.08 Å). We introduce, as discussed in Ref. 38, a cut-off distance R_c beyond which interactions are neglected. The value of R_c for a given pair of atoms i,j is fixed by the relation $R_c(i,j)=1.4\Sigma(i,j)$, where the parameter $\Sigma(i,j)$ is the sum of the corresponding atomic radii[39] (1.76 Å for Ti and 1.11 Å for Si). Then all the above-mentioned distances are included in the calculation.

(ii) In the particular case of TiSi, Si-Si are second neighbors for which $R_c(\mathrm{Si,Si})=3.11$ Å is larger than the actual distance $R(\mathrm{Si,Si})=3.08$ Å. This fact leads us to take in account these second-neighbors interactions in our calculation.

The interactions $V_{\alpha\beta}$ between orbitals α and β on nearest neighbors situated at a distance R_1 are calculated using Harrison's formula[40] together with his set of empirical parameters (Table III)[40,41] where, for α and β different from *d* orbitals,

$$V_{\alpha\beta}=\frac{\hbar^2}{m}\eta_{\alpha\beta}\frac{1}{R_1^2} \tag{4.1}$$

and for α or β equal to *d* orbitals,

$$V_{\alpha\beta}=\frac{\hbar^2}{m}\eta_{\alpha\beta}\left[\frac{r_d^3}{R_1^7}\right]^{1/2}, \tag{4.2}$$

where r_d is a scaling parameter[40] for each transition-metal atom, equal to 1.08 Å for Ti. For next-nearest neighbors for which the distance R is less than R_c, we use the scaling law[38]

$$V_{\alpha\beta}=V_{\alpha\beta}(R_1)\exp\left[-\gamma\left[\frac{R}{R_1}-1\right]\right] \tag{4.3}$$

with $\gamma=2.5$ for α and β different from *d* orbitals and $\gamma=4.0$ for the others. These values give nearly the same logarithmic derivative at R_1 as those given by Harrison but the interactions decrease faster with distance than in Eqs. (4.1) and (4.2).

As the charge transfer on atoms is reduced by self-consistency, we adjust the atomic energy level $E_d(\mathrm{Ti})$ to get strict neutrality on the Ti atom, i.e., to have four valence electrons on each atom in the valence band. The number of electrons on a Si atom can then be written

$$N_{\mathrm{Si}}=2\sum_{\alpha=s,p}\sum_{n,k}f_{n,\underline{k}}|\langle\Phi_\alpha|\Psi_{n,\underline{k}}\rangle|^2 \tag{4.4}$$

where $\Psi_{n,\underline{k}}$ is the Bloch state of wave vector $\underline{k}$ belonging to band n, $f_{n,\underline{k}}$ is the occupancy factor equal to unity for filled bands and zero for empty ones, and Φ_α is a state on Si atoms. The $E_d(\mathrm{Ti})$ values obtained in this way are

TABLE III. Harrison's set of parameters.

$\eta_{ss\sigma}$	$\eta_{sp\sigma}$	$\eta_{pp\sigma}$	$\eta_{pp\pi}$	$\eta_{sd\sigma}$	$\eta_{pd\sigma}$	$\eta_{pd\pi}$
−1.32	1.42	2.22	−0.63	−3.16	−2.95	1.36

-4.86 eV for Ti_5Si_3 ,

-7.86 eV for TiSi ,

and

-7.86 eV for $TiSi_2$.

From this we determine the density of states by using the method of tetrahedra[42] for TiSi and, because of the number of atoms and the complex atomic structure of $TiSi_2$ and Ti_5Si_3, we use for them the method of "special points" in the Brillouin zone.[43] For both methods, the results are found to converge rapidly. Total and partial densities of states calculated in this way are shown in Fig. 9 for the different compounds.

Using these calculated DOS, we can then synthesize Si $L_{2,3}VV$ theoretical ALS $F_T(E)$ for the three silicides using the formula

$$F_T(E)=c_{ss}s*s+c_{sp}s*p+c_{pp}p*p \ , \tag{4.5}$$

where s and p denotes the silicon partial DOS and c_{ij} are weighting coefficients.

The difficulty with the use of formula (4.5) arises from the choice of the various coefficients c_{ij} for which no reliable first-principles calculation exists. However, we can try to infer them from previous work on the Si $L_{2,3}VV$ Auger line from which we can distinguish two extreme cases. The first is illustrated by pure silicon for which a correct fit to experimental line shapes implies the quasineglect of s-s contributions ($c_{ss}\simeq 0$) and a strongly attenuated contribution of s-p relative to p-p processes ($c_{sp}/c_{pp}\simeq 0.22$).[9] An example of the second case is that of Pd silicides for which s-s and s-p processes play an important role in such a way that the Si line shape can be interpreted directly by the self-folding of the total DOS without any further weighing.[14,15] In this case, the Si $L_{2,3}VV$ Auger line shape gives rise to three or more clearly distinguishable peaks related to the various contributions.

Concerning Ti silicides, as can be seen from experimental spectra (Fig. 1), the situation looks rather like that of Ni or Ca silicides[16,17,21] for which the line shape is only slightly modified with respect to bulk silicon. Now in the case of Ni and Ca silicides, fit of theoretical calculations to experimental data leads, as in bulk silicon, to the predominance of p-p processes over the s-p and s-s ones. So, considering the similarities in line-shape changes between Ti and Ni or Ca silicides, and the fact that a Si $L_{2,3}VV$ line shape with three or more distinguishable peaks has never been reported in the literature for Ti silicides, we decide to choose the various coefficients in formula (4.5) for Ti silicides as those in bulk silicon. Figure

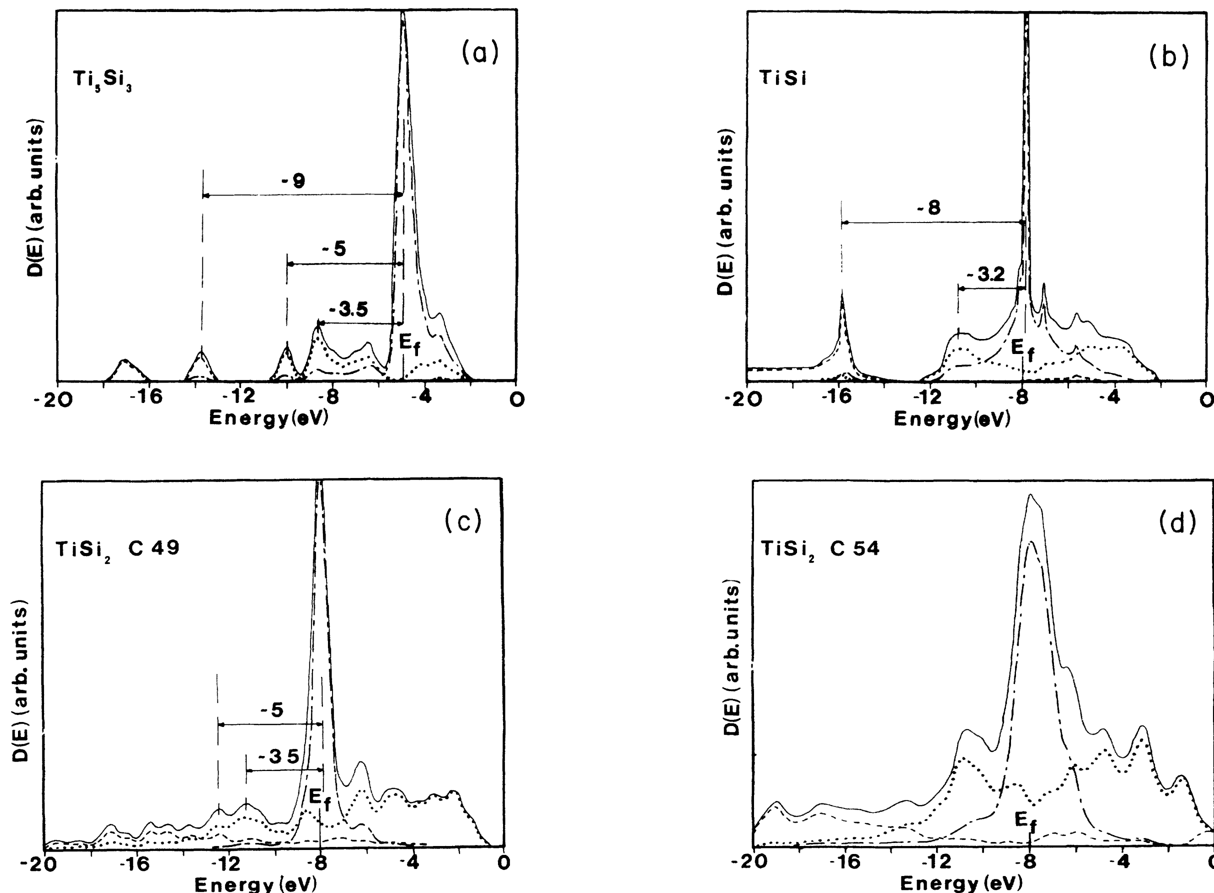

FIG. 9. Theoretical densities of states (DOS) for the three Ti silicides: (a) Ti_5Si_3, (b) TiSi, (c) $TiSi_2$ $C49$, (d) $TiSi_2$ $C54$. Solid line, total DOS; dashed line, s partial DOS; dotted line, p partial DOS; dot-dashed line, d partial DOS.

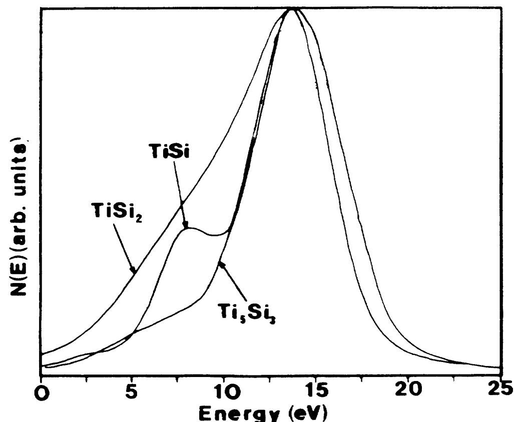

FIG. 10. Theoretical Si $L_{2,3}VV$ Auger line shapes for the three Ti silides calculated as discussed in the text.

10 displays the theoretical Si $L_{2,3}VV$ ALS obtained in this way for the three Ti silicides. No ALS differences have been noted between the two $TiSi_2$ structures.

The calculated DOS can also be used in the interpretation of the ELS spectra. Indeed, Bauer[44] has derived an approximate expression for the number of electrons suffering an energy loss ΔE due to electronic transitions of valence electrons to empty conduction states. If the initial valence-band state is narrow and the transition is isolated in energy from other ones, Ludeke and Esaki[45] have further simplified this expression and obtained

$$I(\Delta E)=\sum_{c} L_{c,v} D_c(\Delta E) , \qquad (4.6)$$

where c and v refer to conduction and valence states, respectively, L_{cv} is the transition probability averaged over all possible momentum changes, and $D_c(\Delta E)$ is the density of empty states in the conduction band. So using the calculated DOS, electronic transition energies can be predicted by energy differences between peaks appearing in the filled valence states density and in the empty conduction states one.

V. DISCUSSION

With the help of the previous theoretical elements, we now turn to the interpretation of our results. We first discuss the high-temperature treatments ($T>400\,°C$) which seem to be the simplest ones before going on with the low-temperature results.

A. Results for $T \geq 400\,°C$

For annealing temperatures higher than 400 °C but less than 500 °C, comparison between experimental and theoretical line shapes leads us to identify the line shape of Fig. 6 as that of $TiSi_2$. Under this assumption, the resistivity value then obtained is about 125 $\mu\Omega$ cm corresponding to the value usually obtained on $C49$ $TiSi_2$ (Ref. 46), and so we can infer that $TiSi_2$ is formed in its $C49$ phase. Turning now to the ELS spectra, the experimentally observed transitions at 3.5 and 5 eV can well be explained by transitions of electrons from initial states related to the features at 3.5 and 5 eV below the Fermi level (E_F) in the theoretical DOS to an empty state near E_F [Fig. 9(c)]. The supposition of a single final state near E_F is highly suggested by the sharp and intense peak near E_F in the theoretical DOS. Other features in this DOS are either too weak or appear at energies too close to plasmons energies so that they cannot be readily observed on the experimental ELS spectra. So all our results clearly establish the formation of $TiSi_2$ in its $C49$ phase for annealing temperatures in the range 400–500 °C.

For annealing temperatures above 500 °C, the Si $L_{2,3}VV$ ALS lies between that in pure silicon and that in $TiSi_2$. Combined with the observed double plasmon losses, the appearance of the diffraction diagram of the substrate, and the evolution of the Auger intensities, this is consistent with the disruption of the previously formed $TiSi_2$ film and $TiSi_2$ grains formation on the substrate. On ELS spectra, the transitions at 3.5 and 5 eV are associated, as in the previous case, with the presence of $TiSi_2$, whereas the feature at 8 eV is explained by the silicon S_2 surface transition.

As regards the deposition of Ti on a 400 °C heated Si substrate, the results are very similar to the annealing case for temperatures above 500 °C, and once again we can conclude to the formation of $TiSi_2$ grains on the Si substrate. This is clearly evidence by the electron transmission microscopy result and the overall agreement between this observation and the results deduced from spectroscopic measurements demonstrates the accuracy of our analysis.

B. Low-temperature results

1. Room-temperature deposition

The comparison between experimental and theoretical line shapes shows that the extra feature appearing in the experimental curve at $\simeq 6$ eV from the main peak is related to the formation of TiSi. However, this secondary peak seems less pronounced on the experimental spectra than on the theoretical ones and so we cannot exclude from this first examination the formation of Ti_5Si_3 too. As regards ELS spectra, the feature at $\simeq 7.5$ eV can be interpreted by the peak at $\simeq 8$ eV below the Fermi level in the TiSi DOS [Fig. 9(b)] as well as by the feature at $\simeq 9$ eV in the Ti_5Si_3 DOS [Fig. 9(a)]. The feature at $\simeq 3.5$ eV agrees rather well with the predicted peaks at 3.5 eV in the Ti_5Si_3 theoretical DOS and with the 3.2-eV peak in the TiSi one. On the contrary, the peak at $\simeq 5$ eV has only a corresponding structure in the Ti_5Si_3 DOS but not in the TiSi one. This observation clearly suggests the presence of Ti_5Si_3 together with TiSi. In order to complete the above discussion, we can also look at the Si $L_{2,3}VV$ intensity and line-shape differences in the three main possible cases of interest here, assuming the formation of TiSi and/or Ti_5Si_3 up to a deposited amount of $\simeq 5\times10^{15}$ atoms/cm^2 as indicated by the ELS spectra: (1) formation of TiSi only; (2) formation of TiSi followed

by the formation of Ti_5Si_3; (3) simultaneous formation of TiSi and Ti_5Si_3 in a mixture. Concerning the first case, Fig. 11 shows that the simulation of the 2D growth of TiSi alone until deposition of $\simeq 5\times 10^{15}$ atoms/cm^2 is not in good agreement with the experimental Auger intensities. It can be noted that the agreement would be still worse with a 3D growth. So, formation of TiSi alone cannot explain our results. However, due to the experimental uncertainties in Auger intensities, it is more difficult to choose between the last two cases. Nevertheless, an interesting way of proceeding is to take into account the Auger intensities to make linear combinations F_{LC} of theoretical Auger line shapes F_T in the different silicides for comparison with the experimental ones in order to find the best agreement. The general expression for this type of linear combination is

$$F_{LC}=a_{Si}F_T(Si)+a_{Ti_5Si_3}F_T(Ti_5Si_3)+a_{TiSi}F_T(TiSi)+a_{TiSi_2}F_T(TiSi_2)\ , \tag{5.1}$$

where the a_i are coefficients whose values are given by quantitative considerations.

Considering the growth of TiSi followed by that of Ti_5Si_3 [case (2)], we can assume the 2D growth of TiSi until deposition of $(2-2.5)10^{15}$ atoms/cm^2 according to Fig. 11. At this point, the silicon Auger intensity would be the sum of the substrate signal attenuated by the TiSi layer and of the silicon in the TiSi layer:

$$I_{Si}(2\times 10^{15}\text{ Ti atoms/cm}^2)=I_{Si}(\text{substrate})k^n+I_{Si}(\text{TiSi})(1-k^n)\ , \tag{5.2}$$

where k is the intensity attenuation factor for a TiSi monolayer and n is the number of monolayers in the TiSi layer. Taking into account the TiSi mass density (4.32 g/cm^3) and atomic density (1.68×10^{15} atoms/cm^2), the value of n for 2×10^{15} deposited Ti is about 3. With the attenuation length values estimated from Seah and Dench,[27] k is about 0.6. Finally, the silicon Auger signal in TiSi with respect to pure silicon is about 0.58, different from 0.5 because of densities and attenuation lengths differences.[29] With these numerical values, the different coefficients in Eq. (5.1) for normalized ALS, i.e., ALS with the same arbitrary fixed amplitude, are

$$a_{Si}=0.33,\quad a_{Ti_5Si_3}=0\ ,\qquad a_{TiSi}=0.67,\quad a_{TiSi_2}=0\ . \tag{5.3}$$

Comparison between the calculated line shape using (5.3) and the experimental one at 4-Å-deposited Ti (Fig. 12) shows a relatively poor agreement and, particularly, the TiSi contribution seems overestimated. This demonstrates that at the early stages of the interface formation, Ti_5Si_3 is present together with TiSi as supposed in the third hypothesis. In this case, the total Auger intensity can be expressed as

$$I_{Si}(2\times 10^{15}\text{ Ti atoms/cm}^2)=I_{Si}(\text{substrate})k^n+[\alpha I_{Si}(\text{TiSi})+\beta I_{Si}(Ti_5Si_3)](1-k^n)\ , \tag{5.4}$$

where α and β are the mixture proportions of TiSi and Ti_5Si_3, respectively, $\alpha+\beta=1$, $I_{Si}(\text{TiSi})=0.58$, and $I_{Si}(Ti_5Si_3)=0.42$. Moreover, as there are 0.84×10^{15} Ti atoms per cm^2 in TiSi and 1×10^{15} in Ti_5Si_3, the conservation law for Ti atoms gives

$$(0.84\times 10^{15}\alpha+1\times 10^{15}\beta)n=2.2\times 10^{15}\ . \tag{5.5}$$

As the silicon Auger intensity at $\simeq 4$ Å is 0.67, the best value of α that fulfills these physical constraints is 0.6, which gives for the coefficients of Eq. (5.1) and for normalized ALS

$$a_{Si}=0.44,\quad a_{Ti_5Si_3}=0.18\ ,\qquad a_{TiSi}=0.38,\quad a_{TiSi_2}=0\ . \tag{5.6}$$

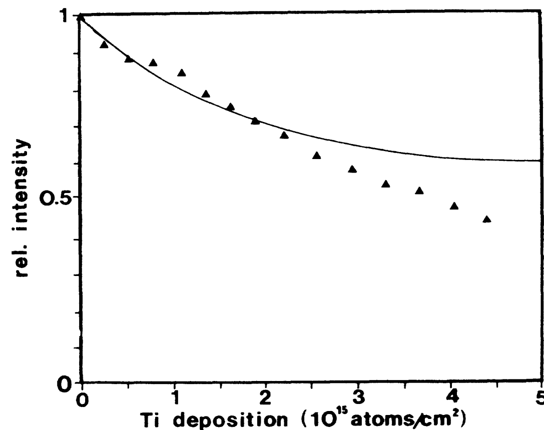

FIG. 11. Comparison between the experimental evolution of the Si $L_{2,3}VV$ Auger intensity during room-temperature deposition of titanium and the simulation of a layer by layer growth of TiSi.

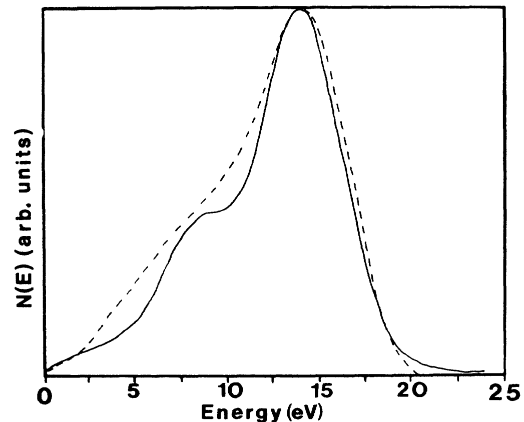

FIG. 12. Comparison between the experimental Si $L_{2,3}VV$ Auger line shape after deposition of 2×10^{15} atoms/cm^2 and the calculated one assuming the growth of TiSi at the early stages of the deposition at 25 °C.

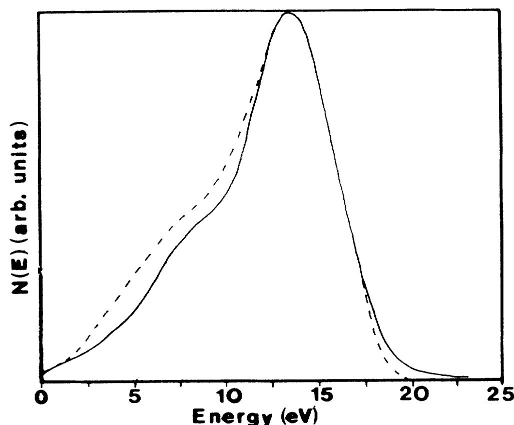

FIG. 13. Comparison between the experimental Si $L_{2,3}VV$ Auger line shape after deposition of 2×10^{15} atoms/cm^2 and the calculated one assuming the growth of a mixture of TiSi and Ti_5Si_3 at the early stages of the deposition at 25 °C.

Figure 13 shows the calculated line shape using the set of coefficients (5.6) together with the experimental one. We can note a better agreement in this case than in that depicted in Fig. 12. The same kind of agreement is obtained between the three experimental ALS of Fig. 1 and the corresponding calculated ALS within the model. Nevertheless, the agreement between the theoretical and experimental ALS is semiquantitative and then the mixture composition deduced (60mol% TiSi, 40mol% Ti_5Si_3) must be considered as indicative. However, if variations of the coefficient values used in the building of theoretical ALS can alter the resulting mixture composition, the main result remains, i.e., the formation of Ti_5Si_3 together with TiSi.

2. *Low-temperature annealings: $T\simeq300$ °C*

Quantitative Auger analysis and ELS results could be consistent with the formation of TiSi after a 250–300 °C annealing. However, the experimental Si $L_{2,3}VV$ ALS in this case [Fig. 6(a)] does not agree with the calculated one for TiSi (Fig. 10) and, moreover, the 5-eV peak on the ELS spectra (Fig. 7) cannot be explained by the theoretical TiSi DOS. To overcome this disagreement, it is possible to suppose the formation of a mixture of Ti_5Si_3, TiSi, and $TiSi_2$. Nevertheless, 300 °C seems a rather low temperature to allow the presence of $TiSi_2$, for which temperature formation is generally reported above 400–500 °C.[1,2] Moreover, in this case, one could suppose the mean composition of the mixture to vary with the annealing time towards Si-rich compounds. However, we have not noted any evolution of the Auger intensities during long-time annealings of several hours.

A better understanding can be achieved if one considers grain boundaries diffusion. Indeed, this mechanism has been supposed to play an important role in the low-temperature reactivity of the Ti-Si system.[47] In this case, the saturated intensities of the Auger signals would be associated with the fact that diffusion at the grain boundaries is inhibited due to the presence of silicon at the surface of the sample. Lattice diffusion, for which the activation energy is generally larger than for grain boundaries diffusion, would occur inside the grains but at a slower rate in such a way that the corresponding changes of the Auger intensities would not be detectable within the time scale under consideration. Taking then into account a small amount of silicon segregation at the surface together with the formation of a mixture of TiSi and Ti_5Si_3 can explain our results.

The decomposition of the Auger intensity corresponding to this model and using the same notation as above is

$$I_{Si}=I_{Si}(Si)(1-k)\Theta+[\alpha I_{Si}(Ti_5Si_3)+\beta I_{Si}(TiSi)][\Theta k+(1-\Theta)] \quad (5.7)$$

where Θ is the silicon surface coverage. The best agreement then obtained with formula (5.7) is with $\Theta=0.55$ and $\alpha=0.6$. Figure 14 shows the agreement obtained with these values between the calculated ALS and the experimental one, which supports the overall validity and coherency of our model.

Finally, let us make a comment on the use of the Si $L_{2,3}VV$ Auger line shape. Of course, we cannot ensure that the coefficient values we choose for the building of the theoretical ALS are the exact ones. However, slight variations of these values does not significantly change our results and main conclusions. On the other hand, taking into account the experimental ALS we get which are only slightly different from that in pure silicon, it is clear that they cannot be explained by the self-folding of the total DOS, as in the Pd-Si case.[14,15] Indeed, in this case, the ALS should exhibit three or more distinguishable peaks corresponding to the various contributions, which is not the case of the ALS obtained here. So, for Ti silicides, the coefficient values used for pure silicon seem quite adequate to describe the experimental results. Nevertheless, doing so, the agreements obtained between the experimental and calculated ALS remain rather semiquantitative, but it is more or less unavoidable considering the complexity of the Auger process. So we have limited our study of the ALS to the comparison of the general trends and main features appearing in the experimen-

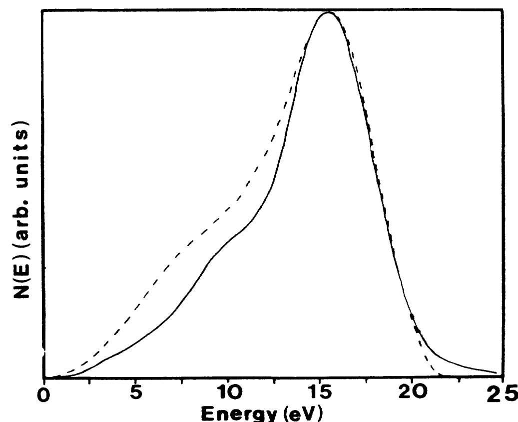

FIG. 14. Comparison between the experimental Si $L_{2,3}VV$ Auger line shape after a 300 °C annealing and the calculated one assuming the formation of a mixture of TiSi and Ti_5Si_3 with a small amount of silicon segregation (see text).

tal ALS on one hand and in the calculated ones on the other hand. Consequently, the quantitative information deduced with the help of the ALS study must be seen as indicative. Finally, it is clear that the ALS alone are not sufficient to test the validity of a model. That is why in each case we have other experimental evidence from ELS, LEED, or resistance data of the model we propose. It is only the coherency between this whole set of experimental results which allows us to give a precise description of the phenomena involved.

VI. CONCLUSION

In this work, we have shown that the Ti-Si interface is reactive even at room temperature with formation of a mixture of TiSi and Ti_5Si_3 at the interface. Upon annealing, different temperature regions have been separated. For $T \simeq 300\,°C$, grain-boundaries diffusion of silicon plays an important role and there is again formation of a mixture of TiSi and Ti_5Si_3. $TiSi_2$ formation is only observed for temperatures above 400 °C. The film is continuous for temperatures below 500 °C and the phase formed is the metastable or $C49$ one. Annealing further to convert the film into the stable $C54$ phase results in the disruption of the previous film and the formation of grains on the substrate, which evidences the importance of nucleation phenomena during the growth of $TiSi_2$ $C54$. $TiSi_2$ grains formation is also observed when depositing Ti on a 400 °C heated Si substrate. Finally, the combination of the techniques used, including the Auger line-shape analysis, has proven to be very powerful in order to get a precise description of the local chemical environment.

ACKNOWLEDGMENTS

We thank Dr. P. Friedel for fruitful discussions and Dr. A Rocher for the transmission-electron-microscopy observations.

[1]G. G. Bentini, R. Nipoti, A. Armigliato, M. Berti, A. V. Drigo, and C. Cohen, J. Appl. Phys. **57**, 270 (1985).
[2]R. Beyers and R. Sinclair, J. Appl. Phys. **57**, 5240 (1985).
[3]R. Butz, G. W. Rubloff, T. Y. Tan, and P. S. Ho, Phys. Rev. B **30**, 5421 (1984).
[4]J. Vahakangas, Y. U. Idzerda, E. D. Williams, and R. L. Park, Phys. Rev. B **33**, 8716 (1986).
[5]E. J. Van Loenen, A. E. M. J. Fischer, and J. F. Van Der Veen, Surf. Sci. **155**, 65 (1985).
[6]S. A. Chambers, D. M. Hill, F. Xu, and J. H. Weaver, Phys. Rev. B **35**, 634 (1987).
[7]J. J. Lander, Phys. Rev. **91**, 1382 (1953).
[8]J. E. Houston, G. Moore, and M. G. Lagally, Solid State Commun. **21**, 879 (1977).
[9]T. Kunjunny and D. K. Ferry, Phys. Rev. B **24**, 4593 (1981); **24**, 4604 (1981).
[10]P. J. Feibelman and E. J. McGuire, Phys. Rev. B **17**, 690 (1978).
[11]D. E. Ramaker, F. L. Hutson, N. H. Turner, and W. N. Mei, Phys. Rev. B **33**, 2574 (1986).
[12]G. A.. Sawatzky, Phys. Rev. Lett. **39**, 504 (1977).
[13]D. R. Jennison, Phys. Rev. Lett. **40**, 807 (1978).
[14]P. S. Ho, G. W. Rubloff, J. E. Lewis, V. L. Moruzzi, and A. R. Williams, Phys. Rev. B **22**, 4784 (1980).
[15]S. D. Bader, L. Richter, M. D. Brodsky, W. E. Brower, and G. V. Smith, Solid State Commun. **37**, 729 (1981).
[16]U. Del Pennino, P. Sassaroli, S. Valeri, C. M. Bertoni, O. Bisi, and C. Calandra, J. Phys. C **16**, 6309 (1983).
[17]J. Zak and S. D. Bader, Phys. Rev. B **27**, 6649 (1983).
[18]G. Rossi and I. Lindau, Phys. Rev. B **28**, 3597 (1983).
[19]L. Calliari, M. Sancrotti, and L. Braicovitch, Phys. Rev. B **30**, 4885 (1984).
[20]M. Sancrotti, I. Abbati, L. Calliari, F. Marchetti, O. Bisi, A. Iandelli, G. L. Olcese, and A. Palenzona, Phys. Rev. B **37**, 4805 (1988).
[21]M. Sancrotti, I. Abatti, A. Rizzi, L. Calliari, F. Marchetti, and O. Bisi, Surf. Sci. **189/190**, 300 (1987).
[22]A. Ishizaka and Y. Shiraki, J. Electrochem. Soc. **133**, 666 (1986).
[23]E. N. Sickafus, Phys. Rev. B **16**, 1436 (1977).
[24]P. H. Van Cittert, Z. Phys. **69**, 304 (1931).
[25]H. H. Madden and J. E. Houston, J. Appl. Phys. **47**, 3071 (1976).
[26]J. P. Langeron, L. Minel, J. L. Vignes, S. Bouquet, F. Pellerin, G. Lorang, P. Ailloud, and J. Le Hericy, Solid State Commun. **49**, 405 (1984).
[27]M. P. Seah and W. A. Dench, Surf. Int. An. **1**, 2 (1979).
[28]C. J. Powell, Surf. Int. An. **7**, 256 (1985).
[29]X. Wallart, thesis, University of Lille (1988).
[30]J. E. Rowe and H. Ibach, Phys. Rev. Lett. **31**, 102 (1973).
[31]C. Wehenkel and B. Gauthe, Phys. Status Solidi B **64**, 515 (1974).
[32]H. Raether, *Excitation of Plasmons and Interband Transitions by Electrons* (Springer-Verlag, Berlin, 1980).
[33]M. Tanelian and S. Blackstone, Appl. Phys. Lett. **45**, 673 (1984).
[34]A. Rocher, X. Wallart, and M. N. Charasse, *Proceedings of the Materials Research Society Spring Meeting, San Diego, 1989* (MRS, Pittsburgh, 1989).
[35]W. B. Pearson, *A Handbook of Lattice Spacings and Structures of Metals and Alloys* (Pergamon, London, 1967), Vol. 2.
[36]H. Herman and S. Skillman, *Atomic Structure Calculations* (Prentice Hall, Englewood Cliffs, New Jersey, 1963).
[37]J. C. Slater and G. F. Koster, Phys. Rev. **94**, 1498 (1954).
[38]I. Lefebvre, M. Lannoo, G. Allan, A. Ibanez, J. Foucade, J. C. Jumas, and E. Beaurepaire, Phys. Rev. Lett. **59**, 2471 (1987).
[39]E. Clementi, D. L. Raimondi, and W. P. Reinhardt, J. Chem. Phys. **47**, 1300 (1967).
[40]W. A. Harrison, *Electronic Structure and the Properties of Solids* (Freeman, San Francisco, 1979).
[41]W. A. Harrison, Phys. Rev. B **24**, 5835 (1981).
[42]J. Rath and A. J. Freeman, Phys. Rev. B **11**, 2199 (1975).
[43]D. J. Chadi and M. L. Cohen, Phys. Rev. B **8**, 5747 (1973).
[44]E. Bauer, Z. Phys. **224**, 19 (1969).
[45]R. Ludeke and L. Esaki, Phys. Rev. Lett. **11**, 653 (1974).
[46]H. J. M. Van Houtum, I. J. M. M. Raaijmakers, and T. J. M. Menting, J. Appl. Phys. **61**, 3116 (1987).
[47]G. W. Rubloff, R. M. Tromp, and E. J. Van Loenen, Appl. Phys. Lett. **48**, 1600 (1986).